# Coulomb Stress Triggering of the Japan Kyushu M7.0 Earthquake on 15 April 2016

**Wu Jianchao**

[a] *Key Laboratory of Earthquake Geodesy, Institute of Seismology, CEA (Wuhan)*

[b] *Wuhan Institute of Earthquake Engineering(Wuhan)*

[c] *Department of Mechanical Engineering,University of Houston(Houston)*

*e-mail: jianchaowu85@gmail.com*

**Qiao Yueqiang**

[a] *Key Laboratory of Earthquake Geodesy, Institute of Seismology, CEA (Wuhan)*

[b] *Wuhan Institute of Earthquake Engineering(Wuhan)*

*e-mail: 286802782@qq.com*

**Lei Dongning**

[a] *Key Laboratory of Earthquake Geodesy, Institute of Seismology, CEA (Wuhan)*

[b] *Wuhan Institute of Earthquake Engineering(Wuhan)*

*e-mail: 357521555@qq.com*

## ABSTRACT

The 2016 Japan Kyushu M7.0 earthquake occurred near the Ryukyu trench on April, 15. After the main earthquake, 8 aftershocks (M>5) occurred near the epicentral area. To reveal the relationship between the main shock and the aftershocks, based on the focal mechanisms of the aftershocks and finite fault model of the main earthquake, we calculated and got the Coulomb failure stress changes on both nodal planes for each aftershocks. We also calculated the Coulomb stress changes on the focal sources of each aftershocks. Both of the calculation results show that most of the aftershocks occurred in the Coulomb stress increasing area triggered by the M7.0 main earthquake. Therefore, we can conclude that the 8 aftershocks(M>5) were probably triggered by the Coulomb failure stress changes.

KEYWORDS: Kyushu M7.0 earthquake, finite fault model, Coulomb stress, stress triggering, focal mechanisms

# INTRODUCTION

The 2016 Japan Kyushu M7.0 earthquake occurred as a result of a strike-slip fault at 12km depth in the upper crust. Focal mechanisms of this earthquake indicate slip occurred on a right-lateral fault striking northeast, which is corresponding to the trend of Ryukyu Trench[1]. The earthquake occurred 280 kilometers northwest of the Ryukyu Trench, where the Philippine Sea Plate begins its northwestward subduction beneath the Eurasia Plate. Near the Ryukyu Trench, the Philippine Sea Plate converges with Eurasia Plate towards the northwest at a velocity of 55 mm/year (Fig. 1). This subduction zone is characterized by rapid plate convergence and high-level seismicity extending to depths of over 600 km[2].

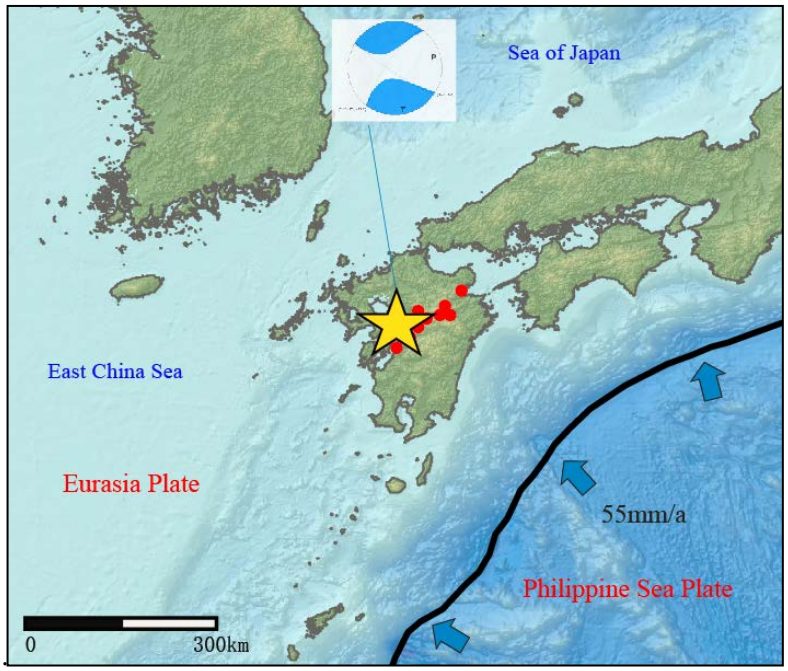


**Figure 1:** The tectonic background of the 2016 Japan Kyushu M7.0 earthquake and aftershocks

Following the M7.0 main earthquake, 8 aftershocks with M >5 occurred till 20 April, 2016. The largest aftershock is M5.7 earthquake, which occurred 20minutes after the main shock. The epicenter is about 15km to the northeast of the main shock. After strong earthquakes occurred, there is often accompanied by a lot of aftershocks. What is the relationship and interaction between the main shock and aftershocks? These questions are currently in the research and debate[3,4]. For the Coulomb stress triggering, the elastic displacement model was established in 1990s[5]. Based on the elastic displacement model of great earthquakes, many researchers could calculate the Coulomb failure stress changes after the strong earthquake[6,7]. Researches on Coulomb stress triggering in recent years show that the main earthquake could change the Coulomb stress on the nearby faults plane and then make the aftershocks easy to occur or delay to occur[8,9].

Previous studies of many earthquake cases show that the increased area of Coulomb failure stress is obviously conducive to the subsequent aftershock occurrence and the decreased area is not conversely[10-14]. Based on the finite fault model of the M7.0 Kyushu earthquake, we calculated the static Coulomb failure stress after this earthquake. Then we discussed the relationship between the coseismic Coulomb stress changes and the aftershocks.

## Coulomb stress Triggering principle

According to the Coulomb-Mohr failure criterion, we assume that the fault plane is developed in the rock and the internal friction coefficient will not change with time. Then, the fault plane will generate shear failure when the shear stress ( $\tau$ ) reach to the frictional strength( $\tau_f$ ). Harris defined ( $\tau$ - $\tau_f$ ) as Coulomb failure stress(CFS)[15]:

$$CFS = \tau - \tau_f = \tau - s - \mu(\sigma_n - p) \tag{1}$$

where $s$ is cohesion and $\mu$ is internal friction coefficient. $\sigma_n$ is normal stress on the fault plane and $p$ is pore pressure. Then the change of Coulomb failure stress is defined as follows:

$$\Delta CFS = \Delta\tau + \mu(\Delta\sigma_n - \Delta p) \tag{2}$$

where $\Delta\tau$ and $\Delta\sigma_n$ are the changes of shear and normal stress respectively. $\Delta p$ is the change of pore pressure. In order to simplify the effect of pore pressure change, assuming that the medium is uniform and isotropic, so the above formula can be transformed into:

$$\Delta CFS = \Delta\tau + \mu'\Delta\sigma \tag{3}$$

where $\mu'$ is apparent friction coefficient and $\mu' = \mu(1-\beta)$ .The theoretical range of $\beta$ is from 0 to 1 . The previous study showed that the changes of $\mu'$ have little effect on the spatial distribution of Coulomb failure stress[6-9]. So we take $\mu'$=0.4 with reference to previous researcher's result in our research.

The Dislocation Theory reveals the relationship between the distribution of stress field on the discontinuous plane and surrounding around in the continuous medium[16]. Based on the geometric parameters of earthquake dislocation plane, we can solve the Coulomb failure stress field in the elastomer's interior. This article adopt the finite element model given by Gavin Hayes[17]. We

studied the Coulomb failure stress changes caused by the M7.0 Kyushu earthquake and revealed its triggering effect to the aftershocks.

To invert the reliable Coulomb failure stress changes, we need to build a more realistic finite fault failure model. In this paper, we adopted the finite element model that had been inverted from GSN broadband waveforms by Gavin Hayes (Fig.2). Gavin Hayes had used GSN broadband waveforms downloaded from the NEIC waveform server and analyzed 45 teleseismic broadband P waveforms, 12 broadband SH waveforms, and 62 long period surface waves selected based on data quality and azimuthal distribution. Waveforms are first converted to displacement by removing the instrument response and are then used to constrain the slip history using a finite fault inverse algorithm.

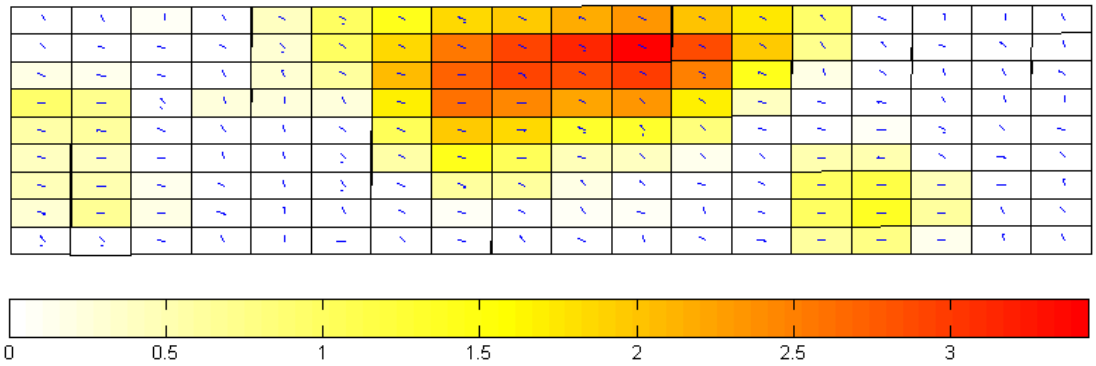


**Figure 2:** The finite fault model of the 2016 Kyushu M7.0 earthquake(unit:m)

## CALCULATION RESULTS AND ANALYSIS

We collected the focal mechanisms of the 8 aftershocks given by USGS. Based on Coulomb3.3 program from USGS, we calculated the Coulomb stress changes on both nodal planes of the 8 aftershocks using the finite element models (Fig.3). We also calculated the Coulomb stress changes on the focal source in the crust (Tab.1). The stress changes on the source point will be more accurate to explain the stress triggering effect of the main M7.0 earthquake.

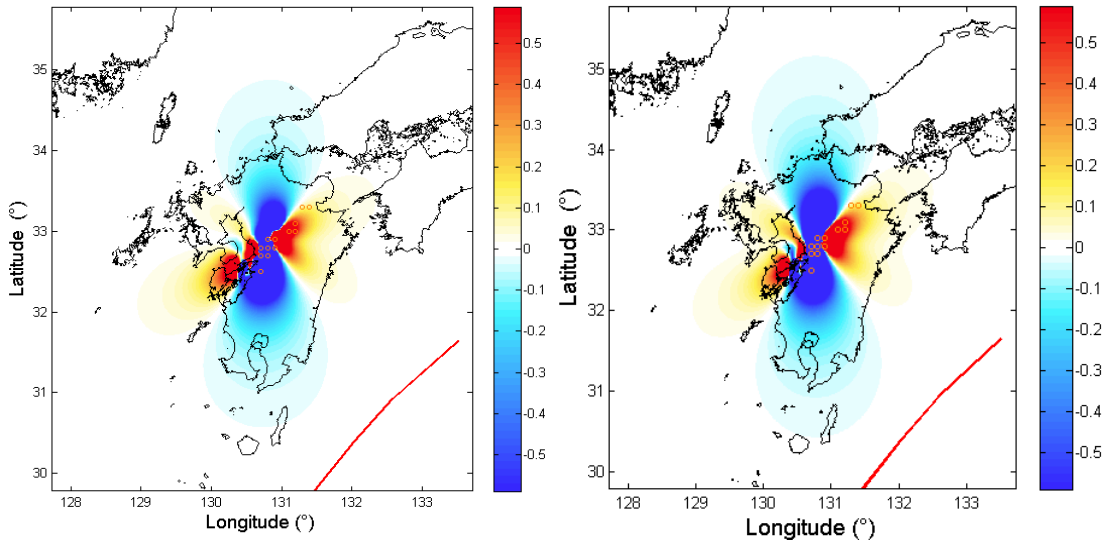


(2016-04-15 M5.7 Left:289,33,-76; Right:93,58,-98)

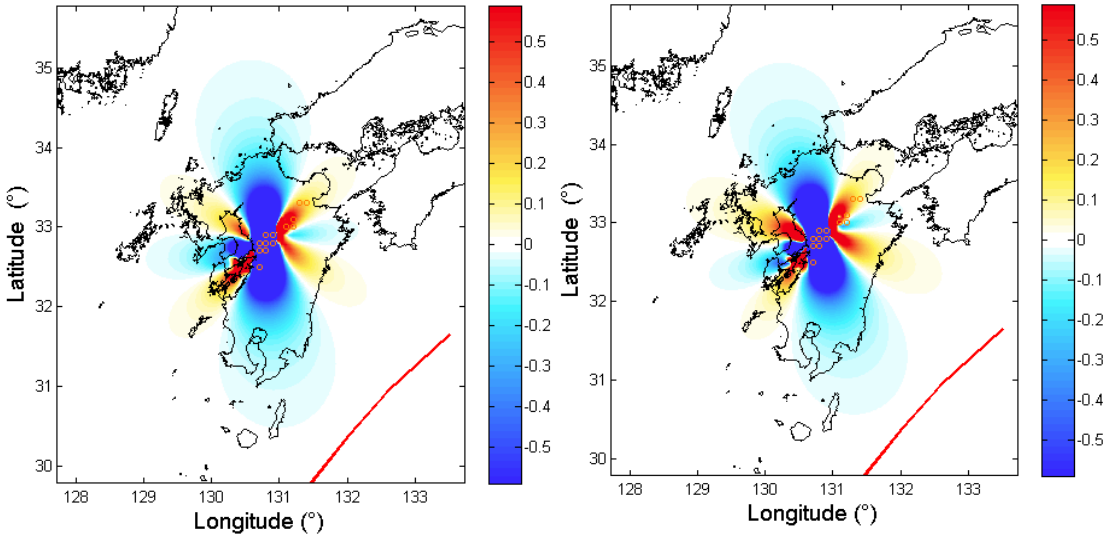


(2016-04-15 M5.4 Left: 296,66,-11; Right:30,79,-156)

**Figure 3:** *Continues…*

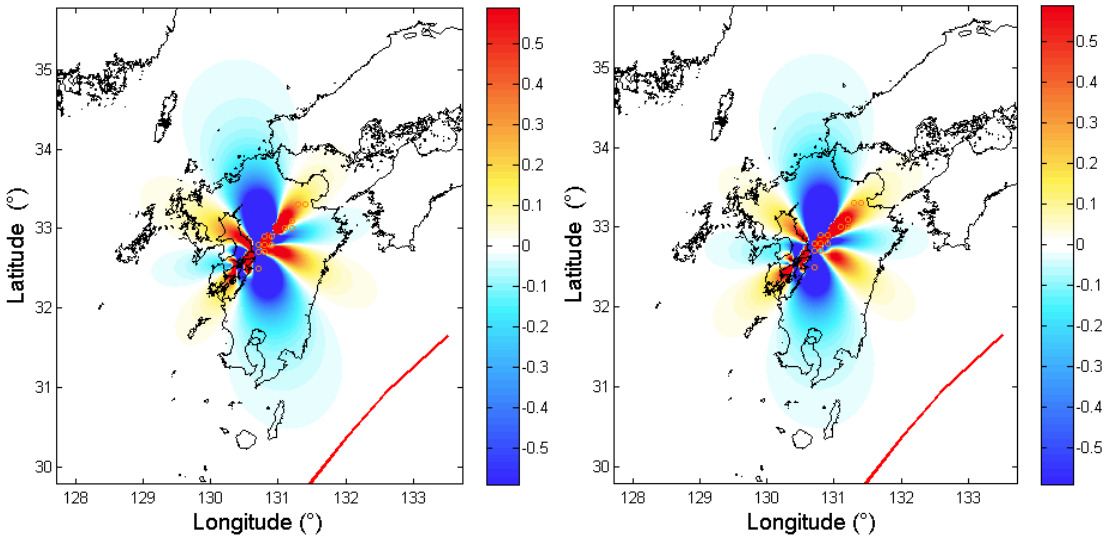


(2016-04-15 M5.5 Left:220,81,-162; Right:127,72,-10)

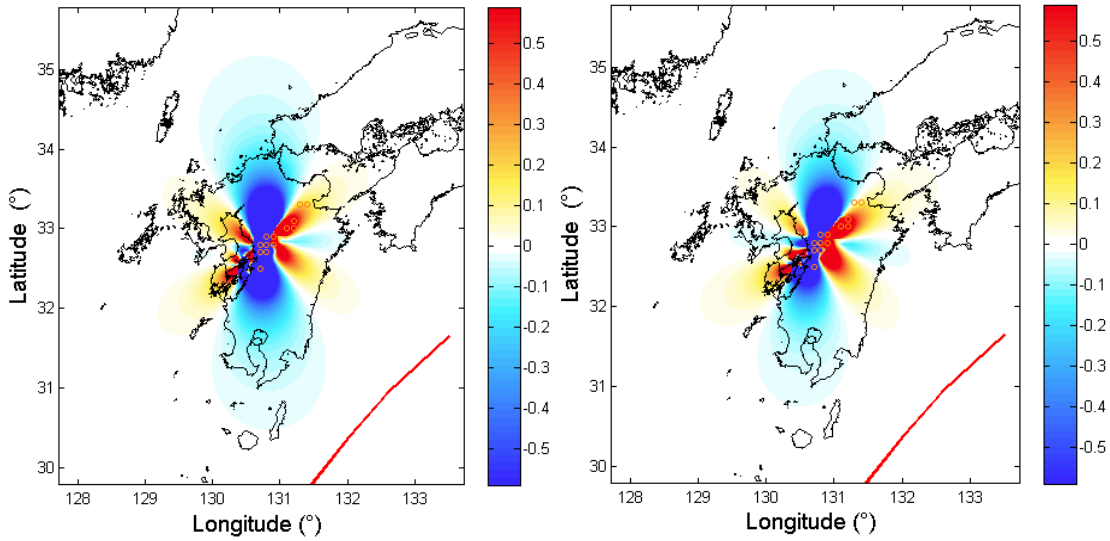


(2016-04-15 M5.1 Left: 245,76,-138; Right:143,49,-18)

**Figure 3:** *Continues…*

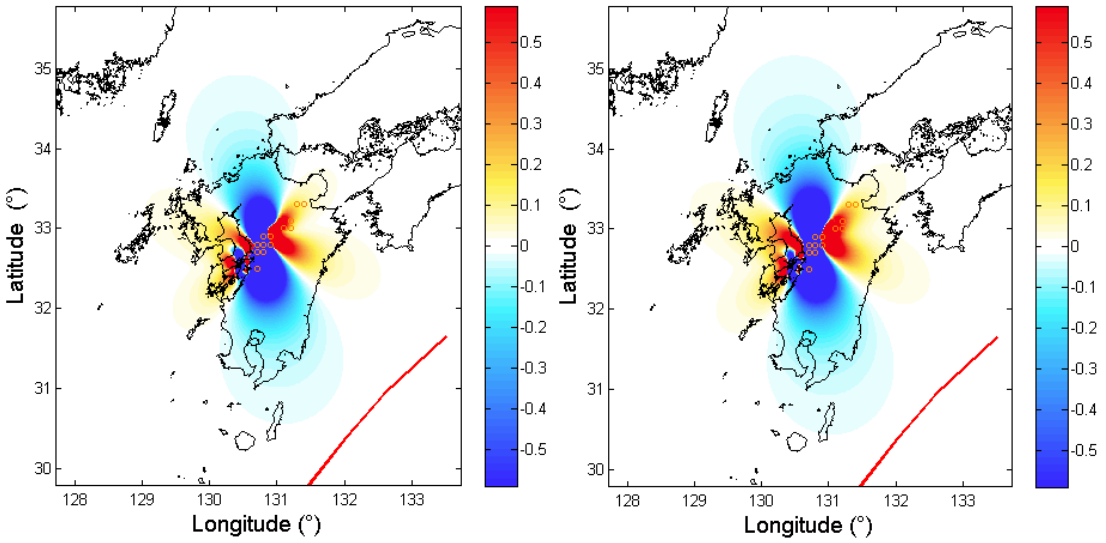


(2016-04-16 M5.2 Left: 242,36,-108; Right:84,56,-77)

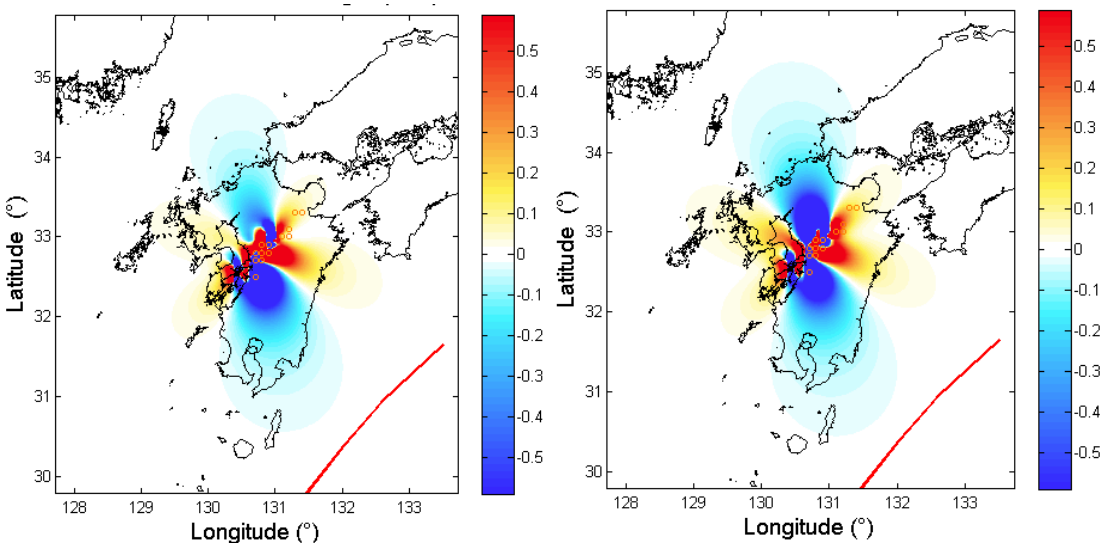


(2016-04-16 M5.3 Left: 242,33,-103; Right:78,58,-81)

**Figure 3:** *Continues…*

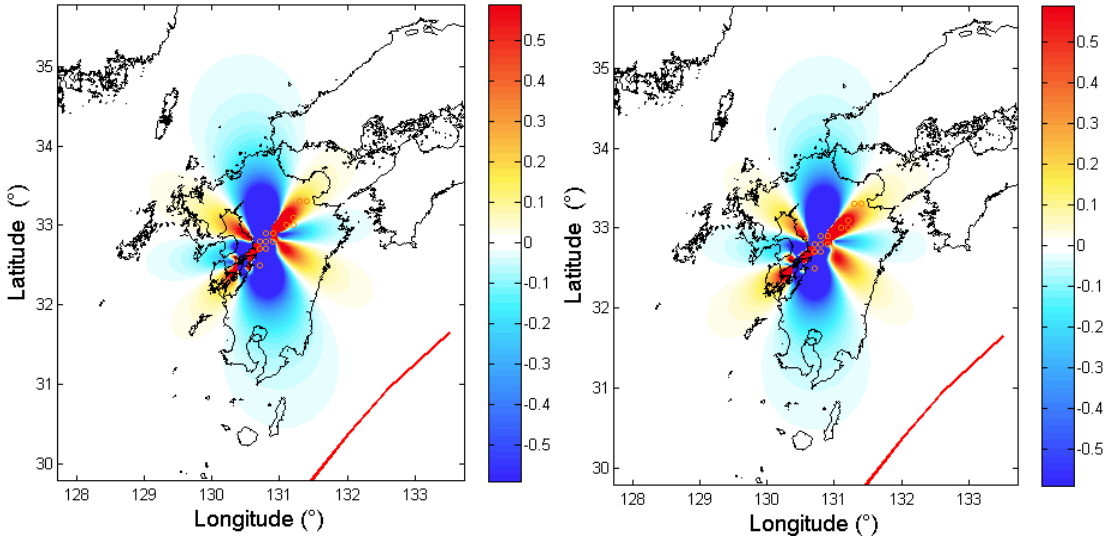


(2016-04-18 M5.3 Left:225,84,-168; Right:133,78,-6)

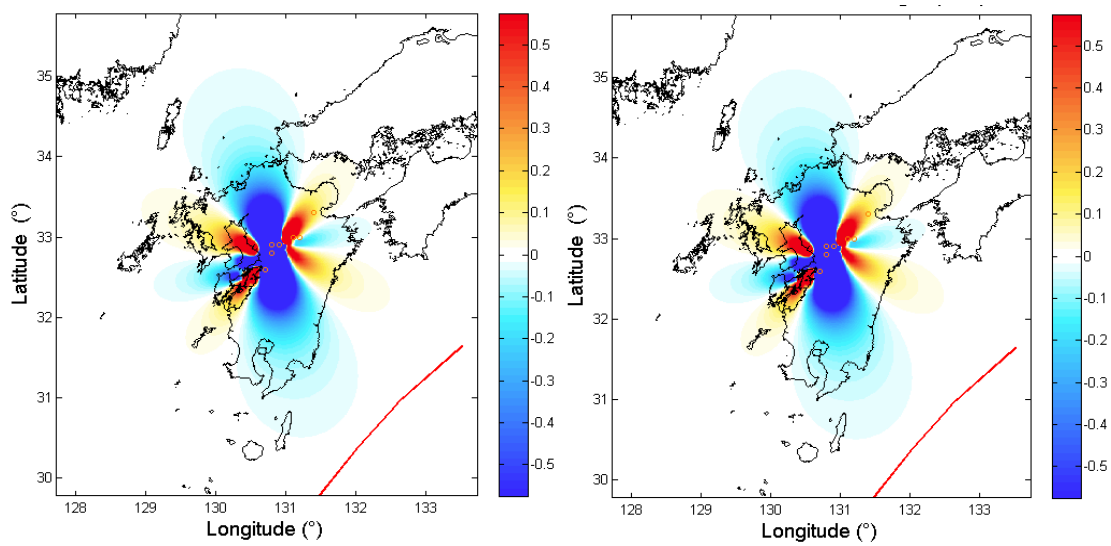


(2016-04-19 M5.1 Left: 123,72,-4; Right:215,86,-161)

**Figure 3:** Coulomb stress changes on both nodal planes of 8 aftershocks triggered by the 2016 Kyushu M7.0 earthquake

From the theory of stress triggering, the receiving faults are used to describe the comprehensive features of the areal faults. Different kinds of receiving faults reflects different corresponding of Coulomb failure stress produced by the main shock. In this paper, we take use of the focal mechanisms of the aftershock, that is inverted by intermediate and long-period body and surface-waves. We consider both of the nodal plane of each aftershock as the receiving faults to make sure that there is no omissions.

We assume that the model is a half-space elastic medium, and the Young's modulus is $8.0\times10^5$ bar. The poisson's ratio is 0.25 and the effective friction coefficient is 0.4. We adopted Coulomb3.3 program to calculate the Coulomb failure stress changes. The stress, produced by the Kyushu M7.0 earthquake on the rupture surface and focal depth of the aftershocks, is essential for us to explore the causes of the large aftershock.

Figure 3 shows the calculated Coulomb failure stress produced by the Kyushu M7.0 earthquake on each fracture plane of the 8 aftershocks. The two figures for each aftershock are different in detail due to representing two nodal planes. Both results show that the increased area and decreased area of Coulomb failure stress appear as a conjugated characteristic. We can conclude that most of the aftershocks occurred in the Coulomb stress increasing area. We can also make a further inference that most of the aftershocks are triggered by the main M7.0 earthquake.

Apart from this calculation, we also calculated the Coulomb stress changes in the focal source of each aftershocks (Tab.2). We can find that the Coulomb stress、shear stress and normal stress increase greatly compared with that before the earthquake occurrence. The results indicate that most of the aftershocks were triggered by the Coulomb stress produced by the c earthquake.

**Table 1:** The basic parameters of the aftershocks and stress calculation results

| Aftershocks | Coordinates (°) | Depth (km) | Fault Plane (°) | Coulomb stress（bar） | Shear stress（bar） | Normal stress（bar） |
|---|---|---|---|---|---|---|
| M5.7 | 32.881<br>130.846 | 10 | 289,33,-76 | -9.545 | -14.776 | -9.545 |
| | | | 93,58,-98 | -53.288 | -4.008 | -123.202 |
| M5.4 | 32.926<br>131.043 | 4.91 | 296,66,-11 | 1.041 | -1.158 | 5.498 |
| | | | 30,79,-156 | -0.079 | -1.163 | 2.711 |
| M5.5 | 32.980<br>131.136 | 13.78 | 220,81,-162 | -0.143 | -0.495 | 0.881 |
| | | | 127,72,-10 | 0.696 | -0.490 | 2.964 |
| M5.1 | 33.282<br>131.398 | 10 | 245,76,-138 | 0.223 | 0.166 | 0.143 |
| | | | 143,49,-18 | 0.161 | 0.165 | -0.008 |
| M5.2 | 32.848<br>130.777 | 9.09 | 242,36,-108 | -10.287 | -5.087 | -13.000 |
| | | | 84,56,-77 | -29.730 | -5.098 | -61.582 |
| M5.3 | 32.747<br>130.668 | 16.2 | 242,33,-103 | -22.650 | -19.444 | -8.015 |
| | | | 78,58,-81 | -13.837 | -20.032 | 15.488 |
| M5.3 | 33.013<br>131.092 | 10.70 | 225,84,-168 | 1.357 | 1.244 | 0.283 |
| | | | 133,78,-6 | 2.232 | 1.213 | 2.546 |
| M5.1 | 32.512<br>130.567 | 3.19 | 123,72,-4 | 1.002 | 2.282 | -3.200 |
| | | | 215,86,-161 | 2.866 | 2.218 | 1.620 |

## DISCUSSION AND CONCLUSION

By using the focal mechanisms of the aftershocks provided by USGS, based on the preliminary finite fault results given by Gavin Hayes, we calculated the Coulomb stress changes after the Kyushu M7.0 earthquake. According to the perspective of faults and earthquakes interaction, we analyzed the relationship between the Kyushu M7.0 earthquake and the M>5 aftershocks.

We calculated the Coulomb failure stress changes on each nodal plane of the M>5 aftershocks. The results show that most of the aftershocks occurred in the Coulomb failure stress increasing area produced by the main M7.0 earthquake. We also calculated the Coulomb failure stress on each focal source of the M>5 aftershocks. Compared with the stress state before the M7.0 earthquake, the Coulomb failure stress on the focal source increased too. It can be concluded that the Coulomb stress changes are probably the important reasons why the strong aftershocks occurred.

## REFERENCES

1. M7.0-1km WSW of Kumamoto-shi, Japan. http://earthquake.usgs.gov/earthquakes/eventpage/us20005iis# general
2. Smoczyk, G.M., Hayes, G.P., Hamburger, M.W., Benz, H.M., Villaseñor, Antonio, and Furlong, K.P., 2013, Seismicity of the Earth 1900–2012 Philippine Sea Plate and vicinity: U.S. Geological Survey Open-File Report 2010–1083-M, scale 1:10,000,000, http://dx.doi.org/10.3133/ofr20101083m.
3. Wu Jianchao, Lei Dongning,Cai Yongjian. Stress triggering of the 2012Sumatra M8.2 earthquake by the 2012 Sumatra M8.6 earthquake. Vol.20,2015
4. Zhou Longquan, Ma Hong-sheng, Xia Hong, et al. Large aftershocks triggering by Coulomb failure stress following the 2007 Ms8.5 and 8.3 Sumatra great earthquakes. Earthquake. 2008,28(1):41-43
5. Okada Y., Internal deformation due to shear and tensile faults in a half-space. Bull. Seis. Soc. Am., 1992,82:1018-1040.
6. Wu Jianchao, Yu Song, et al. Stress triggering of the Lushan M7.0 earthquake by the Wenchuan Ms8.0 earthquake. Geodesy and Geodynamics.2013,4(3):35-39
7. Fred F. Pollitz, Ross S. Stein, et al. The 11 April 2014 east Indian Ocean earthquake triggered large aftershocks worldwide. Nature.2012,490:250-252
8. Shinji Toda, Jian Lin, et al. 12May 2008M = 7.9 Wenchuan, China, earthquake calculated to incr ease failur e stre ss and seismicity rate on three major fault systems. Geophysical Research Letters.2008.35:1-6

9. Lin, J. and R.S. Stein. Stress triggering in thrust and subduction earthquakes and stress interaction between the southern San Andreas and nearby thrust and strike-slip faults. Journal of Geophysical Research, 2004. 109, B02303:1-19.

10. Ji, C., D.J. Wald, and D.V. Helmberger, Source description of the 1999 Hector Mine, California earthquake; Part I: Wavelet domain inversion theory and resolution analysis, Bull. Seism. Soc. Am., Vol 92, No. 4. pp. 1192-1207, 2002.

11. Bassin, C., Laske, G. and Masters, G., The Current Limits of Resolution for Surface Wave Tomography in North America, EOS Trans AGU, 81, F897, 2000.

12. Ji, C., D. V. Helmberger, D. J. Wald, and K. F. Ma (2003), Slip history and dynamic implications of the 1999 Chi-Chi, Taiwan, earthquake, J Geophys Res-Sol Ea, 108(B9).

13. Shao, G. F., X. Y. Li, C. Ji, and T. Maeda (2011), Focal mechanism and slip history of the 2011 M-w 9.1 off the Pacific coast of Tohoku Earthquake, constrained with teleseismic body and surface waves, Earth Planets Space, 63(7), 559-564.

14. Lei Dongning, Wu Jianchao, Cai Yongjian, Li Heng, and Hu Qing: "Coseismic Coulomb Stress Change of Japan Mw9.0 Earthquake and Triggering of Aftershocks" Electronic Journal of Geotechnical Engineering, 2015(20.4): 1243-1252. Available at ejge.com.

15. Harris R D. Introduction to special section: stress triggers, stress shadows and implications for seismic hazard. Journal of Geophysical Research. 1998,103:24347-24358.

16. Waseim Ragab Azzam: "Seismic Response of Bucket Foundation and Structure Under Earthquake Loading" Electronic Journal of Geotechnical Engineering, 2014 (19.F) pp 1477-1489. Available at ejge.com.

17. Preliminary Finite Fault Results for the Apr 15, 2016 Mw 7.0 1 km WSW of Kumamoto-shi, Japan Earthquake. http://earthquake.usgs.gov/earthquakes/eventpage/us20005iis#finite-fault



***Editor's note.***
This paper may be referred to, in other articles, as:

Wu Jianchao, Qiao Yueqiang, Lei Dongning: "Coulomb Stress Triggering of the Japan Kyushu M7.0 Earthquake on 15 April 2016" *Electronic Journal of Geotechnical Engineering*, 2016(21.16), pp 5429-5439. Available at ejge.com.